Light-triggered Disassembly of Amyloid Fibrils

Thomas J. Measey and **Feng Gai**[*]
Department of Chemistry, University of Pennsylvania, Philadelphia, PA 19104, USA

Abstract

There is growing demand for novel methods that could render controlled disassembly of higher-order structures formed, for example, by peptides. Herein, we demonstrate such a method based on the application of a photocaged variant of the amino acid lysine, namely lys(Nvoc). Specifically, we introduce lys(Nvoc) into the primary sequence of the amyloidogenic peptide, $A\beta_{16-22}$, at a position where the native sidechain is known to play a key role in fibril formation via hydrophobic interactions. Both AFM and infrared spectroscopic measurements indicate that the resultant $A\beta_{16-22}$ mutant is able to form fibrils; whereas, more importantly, the fibrils thus formed can be completely disassembled upon irradiation with near-UV light, which cleaves the photolabile Nvoc moiety and triggers the restoration of the lysine sidechain. These results suggest that the generation of a single charge in a highly hydrophobic region of the fibrils is sufficient to promote their dissociation. Thus, we envisage that the current approach will find useful applications wherein controlled structural disassembly or content release is required.

Keywords

Amyloid; Aggregation; Caged amino acid; Disassembly; Phototrigger

INTRODUCTION

Self-assembly of proteins and peptides into amyloid fibrils *in vivo* is often unfavorable because of its intimate connection with many pathological conditions.[1] The same process, however, can be exploited *in vitro* for the generation and fabrication of novel biological materials.[2-5] Examples of the latter include tissue engineering scaffolds,[6,7] conductive nanowires,[8] and devices for controlled drug release.[9] While the self-assembly of peptides into various higher order structures can be triggered and controlled by external signals such as pH, temperature, and light,[3,10] the reversal of such self-assembly processes is rather difficult to achieve. A recent example demonstrated that it is possible to use an azobenzene linker to trigger the self-assembly and disassembly processes of certain peptides via the mechanism of photoisomerization.[11-12] Herein, we show that photocaged amino acids can also be employed to control the disassembly of amyloid fibrils using light as a trigger.

Photocaged amino acids are unnatural amino acids containing a covalently bonded photocleavable moiety attached to the sidechain.[13-15] Upon irradiation, irreversible photolytic cleavage (decaging) results in the restoration of the 'natural' amino acid. Such species have been employed to study the precise and non-invasive control of spatiotemporal

---

activity in a number of biological and cellular systems.[13-15] For example, Schneider and co-workers[15] have shown that by introducing a photocaged cysteine residue into the sequence of the MAX1 peptide, which is known to spontaneously form hydrogels with an underlying β-sheet-rich fibrillar matrix, it is possible to use light to trigger the self-assembly of this peptide.[16]

Hydrophobic interactions are known to play a key role in peptide self-assembly and amyloid formation.[1,17] Thus, we hypothesize that a simple strategy that could be effective in disassembling preformed peptide aggregates and/or amyloid fibrils is by converting a hydrophobic moiety, which is initially inserted into the amyloidogenic peptide sequence of interest at a strategically important position, into a charged amino acid sidechain. It is anticipated that the unfavorable burial of the resultant charge upon photocleavage in a highly hydrophobic environment would lead to a shift in the equilibrium, in favor of the peptide monomer, and thus amyloid fibril disassembly. To test this hypothesis, we herein employed a photocaged analogue of lysine (Scheme 1), namely lys(Nvoc) (Nvoc = 4, 5-dimethoxy-2-nitrobenzyloxycarbonyl), to phototrigger the disassembly of amyloid fibrils formed by a mutant of $A\beta_{16-22}$ (sequence KLVFFAE). The latter corresponds to a short segment of the amyloid-β (Aβ) peptide associated with Alzheimer's disease, and has been shown to form amyloid fibrils rich in β-sheet secondary structure.[18] Lys(Nvoc) exhibits an intense near-UV absorption band centered at ~350 nm (Figure S1 in Supporting Information), and it has been demonstrated that the Nvoc moiety can be photocleaved upon irradiation with near-UV light, resulting in a charged lysine sidechain (Scheme 1).[19]

EXPERIMENTAL SECTION

Materials

D_2O (D, 99.96 %) and deuterium chloride (D, 99.5 %) were purchased from Cambridge Isotope Laboratories (Andover, MA). Fmoc–Lys(4,5–dimethoxy–2–nitro–benzyloxycarbonyl)–OH (Fmoc–Lys(Nvoc)–OH) was purchased from Anaspec, Inc. (Fremont, CA), and used without further purification. Fmoc-protected amino acids were purchased from Advanced Chem Tech (Louiseville, KY). Rink amide resin (Subs. = 0.28) was purchased from Novabiochem (San Diego, CA). Wild-type $A\beta_{16-22}$, $A\beta_{16-22}$-F19K* (F19K*), and $A\beta_{16-22}$-K16K* (K16K*) were synthesized using standard fluoren–9–ylmethoxycarbonyl (Fmoc) chemistry protocol on a PS3 peptide synthesizer from Protein Technologies (Tuscon, AZ), and purified by reverse-phase HPLC (1100 Series; Agilent Technologies, Santa Clara, CA). The identity of the peptides was verified using MALDI-TOF mass spectrometry (Voyager-DE RP, Applied Biosystems, Foster City, CA).

Sample Preparation

Appropriate amounts of the F19K*, K16K*, and wild-type $A\beta_{16-22}$ peptides were first dissolved in a 50/50 mixture of 0.1 M deuterium chloride (DCl) in D_2O/Acetonitrile, and the resulting solution was lyophilized overnight, allowing the removal of residual trifluoroacetic acid (TFA) from the HPLC purification, which absorbs in the amide I' region of the peptide IR spectra. Peptide samples used in the subsequent experiments were prepared by directly dissolving the lyophilized peptide solid in 100% D_2O, and the final pH of all samples was determined. Acidic pH is required due to the poor solubility of F19K* at neutral pH. The concentration of the wild-type $A\beta_{16-22}$ was initially determined via the absorbance of the peptide backbone at 214 nm, using an extinction coefficient of 16,177 M^{-1} cm^{-1}, calculated according to reference (20). The concentrations of F19K* and K16K* were determined via the absorbance of the cage at 350 nm, using an extinction coefficient of 5,485 M^{-1} cm^{-1}. Since the absorptivity of phenylalanine is relatively small, compared to the absorbance of the peptide backbone, a large uncertainty in the concentration of wild-type $A\beta_{16-22}$

determined via this method is expected.[21] Thus, after complete irradiation of the sample, the intensity of the resulting amide I' band was employed to further verify the actual concentration of wild-type $A\beta_{16-22}$, using an extinction coefficient of 800 M^{-1} cm^{-1} at the position of the amide I' band maximum.[22] Thus, the concentrations reported in the manuscript are those determined via the latter method.

FTIR Measurements

FTIR spectra were collected at 25°C on a Nicolet Magna-IR 860 spectrometer at a resolution of 4 cm^{-1}. The sample was injected into an assembled CaF_2 cell that was divided into two compartments (one for the reference, and one for the sample), using a homemade Teflon spacer. This enabled the collection of the sample and reference spectra under identical conditions. An automated translational stage was used to cycle the sample and reference sides into and out of the IR beam, to correct for the slow instrument drift. For each cycle, 8 single-beam spectra were collected on each side, and the final spectra correspond to the average of 32 such cycles. The pathlength of the assembled cell was 52 μm determined via the interference fringes of the empty cell.

AFM Measurements

All AFM experiments were performed in air at room temperature, using a multimode atomic force microscope (Nanoscope IIIa; Digital Instruments, Santa Barbara, CA), equipped with an E-type piezoscanner. 5 μL of sample solution was applied to a freshly-cleaved mica surface for ~5 sec., rinsed with 300 μL MPW, and subsequently dried with a slow stream of N_2 gas. Tapping-mode imaging was carried out with a silicon probe (TESP) from Veeco (Camarillo, CA). Height and deflection images were obtained with a scan rate of 1 Hz, integral gain of 0.4, and a proportional gain of 0.6. Multiple images were obtained for each sample at different locations on the mica substrate, to confirm either the presence or absence of fibrils.

Photocleavage Experiments

Irradiation of samples was carried out by placing the sample in the optical path of the third harmonic output of a pulsed Q-switched Nd/YAG laser (λ = 355 nm). The beam diameter was about 10 mm. The energy per pulse was between 200 – 400 μJ, and the repetition rate was 10 Hz. Thus, the average power at the sample was between 2 – 4 mW. To allow for a direct comparison of FTIR spectra and AFM images of the irradiated sample, both the filled FTIR cell and an aliquot of the stock solution (for AFM) were placed together in the optical path of the 355 nm line, and irradiated for a desired amount of time.

RESULTS AND DISCUSSION

We replaced the first phenylalanine residue (i.e., F19) in $A\beta_{16-22}$ with lys(Nvoc) (hereafter referred to as caged lysine or K*, and the resultant mutant is referred to as F19K*). We chose this location for the following reasons. First, both phenylalanine residues in the $A\beta_{16-22}$ sequence are believed to play an important role in maintaining the fibril architecture via aromatic interactions.[23] Second, the importance of π-π interactions in peptide self-assembly is well documented.[24] Thus, we envisage this mutation to be somewhat conservative, as lys(Nvoc) contains an aromatic moiety. Third, photocleavage of the caged moiety leads to the formation of a charged lysine sidechain in the hydrophobic region of the fibril, which should destabilize the underlying β-sheets via an electrostatic mechanism, in accordance with the negative design principle.[25-27]

As shown (Figure 1), the amide I' bands in the Fourier transform infrared (FTIR) spectra of F19K* (containing ~5% wild-type $A\beta_{16-22}$) collected at different times after sample

preparation indicate that this peptide readily self-assembles to form aggregates rich in antiparallel β-sheets.[28,29] It is interesting to note that in the current case, the high-frequency component of the β-sheet amide I' band is peaked around 1704 cm^{-1}, higher than that typically observed (between 1680 – 1690 cm^{-1}) for other antiparallel β-sheet aggregates.[28] This larger splitting may indicate that the photocage facilitates a tighter packing of neighboring strands.[30,31] Atomic force microscopy (AFM) images of the incubated sample show the presence of typical amyloid fibrils (Figure 2). The mature aggregates are similar in morphology to those formed by the wild-type peptide[18] and, as observed for full-length Aβ$_{1-40}$[32] contain a mixture of both rod-like and twisted fibrils. Taken together, the AFM and FTIR results corroborate our initial hypothesis that the Nvoc group can be incorporated into the compact fibrillar structures, and is non-destructive to amyloid formation. Further AFM and FTIR measurements indicate that F19K* can aggregate alone or co-aggregate with an equal amount of wild type Aβ$_{16-22}$ (see Figures S2 and S3 in Supporting Information), suggestive of the versatility of this system.

To test the effectiveness of photocleavage of the caged moiety on the structural integrity of the fibrils, we irradiated the abovementioned fibril solution with unfocused 355 nm laser pulses for different periods of time. As shown (Figure 3), after ~7 hours of total irradiation time, the amide I' band of the peptide solution is converted to a single band that is characteristic of disordered conformations, suggesting complete dissociation of the underlying β-sheet secondary structures. Using the absorbance at 1620 cm^{-1} as a spectroscopic probe, the time constant of the dissociation kinetics was estimated to be about 1 hour for the current experimental condition (Inset of Figure 3). In addition, AFM images of the fully irradiated sample also show no signs of fibrils, but only amorphous aggregates due to drying of the sample on the substrate (Figure 4). Multiple spots of the mica substrate were checked, and we found no evidence of any remaining fibrils. Taken together, these results confirm our expectation that converting a hydrophobic moiety into a charged one would be effective at significantly perturbing, or even totally disassembling, the highly ordered fibril structures, when this moiety is strategically placed at a location that is important for β-sheet stacking. It should be mentioned, that while a pulsed laser was used in the current study (average power = 2–4 mW) to irradiate the sample, similar results have also been obtained in our laboratory using the output of a Xenon lamp, with a few mW of light arriving at the sample. Perhaps even more important, results obtained from control experiments (Figure S4 in Supporting Information) indicate that light irradiation is not effective for disrupting amyloid fibrils formed by the wild-type Aβ$_{16-22}$ peptide, confirming the notion that the photocleavage of the caged moiety and the concomitant generation of a charge in a hydrophobic environment of the fibril is solely responsible for the subsequent fibril disassembly. What is more, as indicated (Figure 5), this strategy is effective even for disassembling fibrils comprised of a significant amount of the wild-type Aβ$_{16-22}$ peptide, further illustrating its potential applications.

Furthermore, to test our hypothesis that the choice of the location of the photocage in the polypeptide sequence is an important factor in the efficacy of the herein proposed method, we synthesized and tested another mutant, namely K16K*. In this case, removal of the photocage results in the restoration of the wild-type Aβ$_{16-22}$ peptide. As the wild-type peptide is highly amyloidogenic, irradiation of the pre-formed aggregates is expected to have little effect on the integrity of the aggregates. Indeed, the FTIR spectrum of a mixture of K16K* and the wild-type Aβ$_{16-22}$ peptide (molar ratio 3:1) obtained after light irradiation (Figure 6) exhibits only a minimal decrease in the aggregation band relative to the spectrum of the initial (non-irradiated) solution, indicating that the peptide aggregates (or fibrils) remain mostly intact. This control experiment further confirms that the light-triggered disassembly of the amyloid structures formed by F19K* cannot be simply attribute to light-induced heat generation, due to the photochemical reaction of the cage.

While this study has focused on a single model system, namely, Aβ$_{16-22}$, we expect that the method should be easily extended to other amyloidogenic systems. Moreover, potential biotechnological applications can be envisaged, such as triggering the controlled release of a pharmacophore from a fibrillar carrier matrix, or the gentle degradation of the underlying fibrillar scaffold for applications involving tissue engineering. Also, it might be possible to introduce the photocaged species at later stages of the aggregation process to allow for better control of the fibril size distribution, via, e.g. fibril truncation. Furthermore, It would be also interesting, in subsequent studies, to identify the key mechanistic elements of the disassembly pathway, such as the conformational and size distribution of the aggregates at various discrete irradiation times. For example, the latter could be studied via fluorescence correlation spectroscopy (FCS), using an amyloidophilic dye such as thioflavin T (ThT) as the fluorescent probe and an approach employed to study the depolymerization mechanism of serpin polymers.

While it is not a focus of the current study, we would like to speculate that this research might facilitate a potential new avenue of therapeutic intervention for a number of debilitating pathologies, e.g. by incorporating photocaged peptides into *in vivo* amyloid deposits, and using light to trigger the clearance of, for example, amyloid plaques. According to the amyloid hypothesis,[34] such proteinaceous deposits are directly linked to neurodegeneration, although some controversy exists as to whether oligomeric species that form earlier in the process may, in fact, be the toxic species.[1] Since the 355 nm light does not cause radiative damage (photodamage) to cells and the Nvoc moiety is relatively non-toxic,[35] it should be possible to extend this method to *in vivo* experiments. Advances in expanding the genetic code of yeast and mammalian cells to encode for photocaged amino acids should facilitate the translation of this method to *in vivo* studies.[36]

CONCLUSIONS

In summary, we have introduced a novel and facile method to control the disassembly of amyloid fibrils, via phototriggering. To the best of our knowledge, this is the first documented account of using photocaged amino acids as a trigger to reverse the amyloid aggregation process. The photocaged variant of the Aβ$_{16-22}$ peptide, F19K*, is able to self-assemble, resulting in fibrillar structures with similar morphologies to those of the wild-type peptide. Photocleavage of the 'cage' moiety results in the formation of a charge in the hydrophobic region of the intra- and inter-sheet space, and, thus, unfavorable electrostatic interactions that disrupt the β-sheet stacking, and completely dissociate the fibrils. Thus, the generation of a single charge in the otherwise ordered and highly stable hydrophobic region of the fibrils is sufficient to promote their complete disassembly. The mechanism is similar to the negative design principal proposed by Richardson and Richardson, whereby charged residues act as 'structural gatekeepers' in natural β-sheet proteins, as an evolutionary defense against unfavorable and often toxic edge-to-edge aggregation.[27]

Supplementary Material

Refer to Web version on PubMed Central for supplementary material.

Acknowledgments

REFERENCES

(1). Chiti F, Dobson CM. Protein Misfolding, Functional Amyloid, and Human Disease. Ann. Rev. Biochem. 2006; 75:333–366. [PubMed: 16756495]

(2). Cherny I; Gazit E. Amyloid: Not Only Pathological Agents but Also Ordered Nanomaterials. Angew. Chem. Int. Ed. 2008; 47:4062–4069.

(3). Knowles TPJ, Buehler MJ. Nanomechanics of Functional and Pathological Amyloid Materials. Nature Nanotech. 2011; 6:469–479.

(4). Waterhouse SH, Gerrard JA. Amyloid Fibrils in Biotechnology. Aust. J. Chem. 2004; 57:519–523.

(5). Rajagopal K, Schneider J. Self-Assembling Peptides and Proteins for Nanotechnological Applications. Curr. Opin. Struct. Biol. 2004; 14:480–486. [PubMed: 15313243]

(6). Kyle S, Aggeli A, Ingham E, McPherson MJ. Production of Self-Assembling Biomaterials for Tissue Engineering. Trends Biotechnol. 2009; 27:423–433. [PubMed: 19497631]

(7). Holmes TC, de Lacalle S, Su X, Liu G, Rich A, Zhang S. Extensive Neurite Outgrowth and Active Synapse Formation on Self=Assembling Peptide Scaffolds. Proc. Natl. Acad. Sci. U. S. A. 2000; 97:6728–6733. [PubMed: 10841570]

(8). Scheibel T, Parthasarathy R, Sawick G, Lin X-M, Jaeger H, Lindquist SL. Conducting Nanowires Built by Controlled Self-Assembly of Amyloid Fibers and Selective Metal Deposition. Proc. Natl. Acad. Sci. U. S. A. 2003; 100:4527–4532. [PubMed: 12672964]

(9). Maji SK, Schubert D, Rivier C, Lee S, Rivier JE, Riek R. Amyloid as a Depot for the Formulation of Long-Acting Drugs. PLoS Biol. 2008; 6:e17. [PubMed: 18254658]

(10). Xie J-B, Cao Y, Pan H, Qin M, Yan Z-Q, Xiong X, Wang W. Photo-Induced Fibrils Formation of Chicken Egg White Lysozyme under Native Conditions. Proteins. 2012 Just Accepted (DOI: 10.1002/prot.24132.

(11). Deeg AA, Schrader TE, Kempter S, Pfizer J, Moroder L, Zinth W. Light-Triggered Aggregation and Disassembly of Amyloid-Like Structures. ChemPhysChem. 2011; 12:559–562. [PubMed: 21344593]

(12). Waldauer SA, Hassan S, Paoli B, Donaldson PM, Pfister R, Hamm P, Caflisch A, Pellarin R. Photocontrol of Reversible Amyloid Formation with Minimal-Design Peptide. J. Phys. Chem. B. 2012 Just Accepted (DOI: 10.1021/jp305311z).

(13). Lemke EA. Precision Control of Cellular Pathways with Light. ChemBioChem. 2010; 11:1825–1827. [PubMed: 20687052]

(14). Riggsbee CW, Deiters A. Recent Advances in the Photochemical Control of Protein Function. Trends in Biotechnol. 2010; 28:468–475.

(15). Mayer G, Heckel A. Biologically Active Molecules with a "Light Switch". Angew. Chem. Int. Ed. 2006; 45:4900–4921.

(16). Haines LA, Rajagopal K, Ozbas B, Salick DA, Pochan DJ, Schneider JP. Light-Activated Hydrogel Formation via the Triggered Folding and Self-Assembly of a Designed Peptide. J. Am. Chem. Soc. 2005; 127:17025–17029. [PubMed: 16316249]

(17). Kim W, Hecht MH. Generic Hydrophobic Residues are Sufficient to Promote Aggregation of the Alzheimer's Aβ42 Peptide. Proc. Natl. Acad. Sci U. S. A. 2006; 103:15824–15829. [PubMed: 17038501]

(18). Balbach JJ, Ishii Y, Antzukin ON, Leapman RD, Rizzo NW, Dyda F, Reed J, Tycko R. Amyloid Fibril Formation by Aβ$^{16-22}$, a Seven-Residues Fragment of the Alzheimer's β-Amyloid Peptide, and Structural Characterization by Solid State NMR. Biochemistry. 2000; 39:13748–13759. [PubMed: 11076514]

(19). Rusiecki VK, Warne SA. Synthesis of N_α-Fmoc-N_e-Nvoc-Lysine and Use in the Preparation of Selectively Functionalized Peptides. Bioorg. Med. Chem. Lett. 1993; 3:707–710.

(20). Kuipers BJH, Gruppen H. Prediction of Molar Extinction Coefficients of Proteins and Peptides Using UV Absorption of the Constituent Amino Acids at 214 nm To Enable Quantitative Reverse Phase High-Performance Liquid Chromatography-Mass Spectrometry Analysis. J. Agric. Food Chem. 2007; 55:5445–5451. [PubMed: 17539659]

(21). Mukherjee S, Chowdhury R, Gai F. Effect of Dehydration on the Aggregation Kinetics of Two Amyloid Peptides. J. Phys. Chem. B. 2009; 113:531–535. [PubMed: 19132862]

(22). Kim YS, Hochstrasser RM. Dynamics of Amide-I Modes of the Alanine Dipeptide in D_2O. J. Phys. Chem. B. 2005; 109:6884–6891. [PubMed: 16851775]

(23). Inouye H, Gleason KA, Zhang D, Decatur SM, Kirschner DA. Differential Effects of Phe19 and Phe20 on Fibril Formation by Amyloidogenic Peptide Aβ16-22 (Ac-KLVFFAE-NH_2). Proteins. 2010; 78:2306–2321. [PubMed: 20544966]

(24). Gazit E. A Possible Role for π-Stacking in the Self-Assembly of Amyloid Fibrils. FASEB J. 2002; 16:77–83. [PubMed: 11772939]

(25). Otzen DE, Kristensen O, Oliveberg M. Designed Protein Tetramer Zipped Together with a Hydrophobic Alzheimer Homology: A Structural Clue to Amyloid Assembly. Proc. Natl. Acad. Sci. U. S. A. 2000; 97:9907–9912. [PubMed: 10944185]

(26). Thirumalai D, Klimov DK, Dima RI. Emerging Ideas on the Molecular Basis of Protein and Peptide Aggregation. Curr. Opin. Struct. Biol. 2003; 13:1–14.

(27). Richardson JS, Richardson DC. Natural β-Sheet Proteins Use Negative Design to Avoid Edge-to-Edge Aggregation. Proc. Natl. Acad. Sci. U. S. A. 2002; 99:2754–2759. [PubMed: 11880627]

(28). Barth A. Infrared Spectroscopy of Proteins. Biochim. Biophys. Acta. 2007; 1767:1073–1101. [PubMed: 17692815]

(29). Petty SA, Decatur SM. Experimental Evidence for the Reorganization of β-Strands Within Aggregates of the Aβ (16-22) Peptide. J. Am. Chem. Soc. 2005; 127:13488–13489. [PubMed: 16190699]

(30). Lee C, Cho M. Local Amide I Mode Frequencies and Coupling Constants in Multiple-Stranded Antiparallel β-Sheet Polypeptides. J. Phys. Chem. B. 2004; 108:20391–20407.

(31). Schweitzer-Stenner R, Measey TJ. Simulation of IR, Raman and VCD Amide I Band Profiles of Self-Assembled Peptides. Spectroscopy. 2010; 24:25–36.

(32). Malinchik SB; Inouye H, Szumowski KE, Kirschner DA. Structural Analysis of Alzheimer's b(1-40) Amyloid: Protofilament Assembly of Tubular Fibrils. Biophys. J. 1998; 74:537–545. [PubMed: 9449354]

(33). Chowdhury P, Wang W, Lavender S, Bunagan MR, Klemke JW, Tang J, Saven JG, Cooperman BS, Gai F. Fluorescence Correlation Spectroscopy Study of Serpin Depolymerization by Computationally Designed Peptides. J. Mol. Biol. 2007; 369:462–473. [PubMed: 17442346]

(34). Hardy J, Selkoe DJ. The Amyloid Hypothesis of Alzheimer's Disease: Progress and Problems on the Road to Therapeutics. Science. 2002; 297:353–356. [PubMed: 12130773]

(35). Reeve JE, Kohl MM, Rodríguez-Moreno A, Paulsen O, Anderson HL. Caged Intracellular NMDA Receptor Blockers for the Study of Subcellular Ion Channel Function. Comm. Integr. Biol. 2012; 5:240–242.

(36). Young TS, Schultz PG. Beyond the Canonical 20 Amino Acids: Expanding the Genetic Lexicon. J. Biol. Chem. 2010; 285:11039–11044. [PubMed: 20147747]
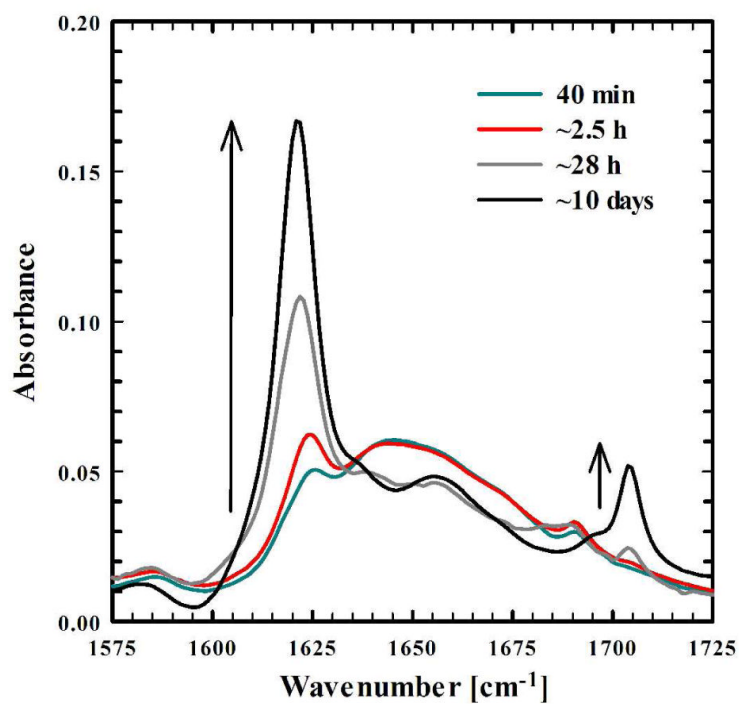
Figure 1.
FTIR spectra (in the amide I' region) of a 1.1 mM mixture of F19K* (95%) and Aβ$_{16-22}$ (5%) in D_2O (pH 2) acquired at different delay times relative to sample preparation, as indicated. The arrows depict the growth of two characteristic spectral features of tightly packed antiparallel β-sheets.[20]
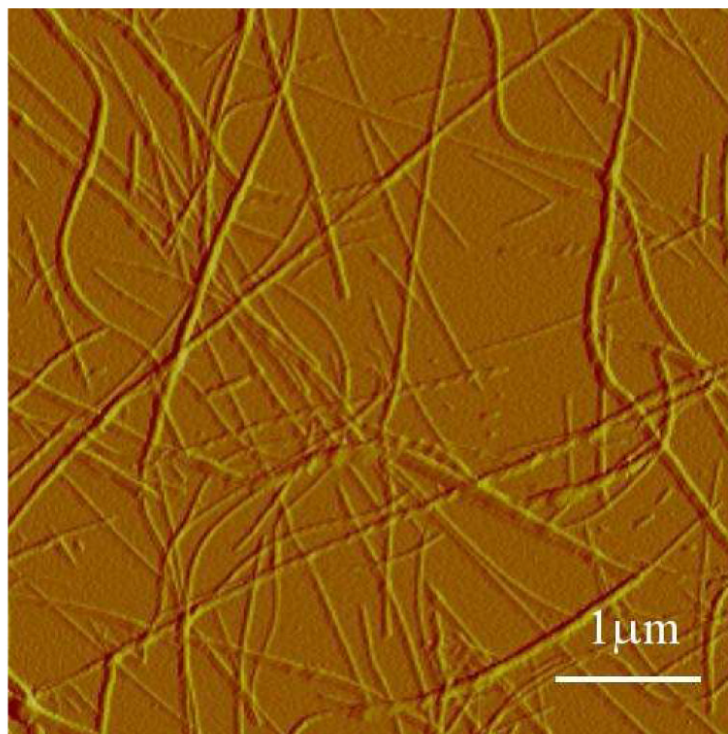
Figure 2.
A representative AFM image of the F19K* solution after 10 days of incubation, showing the formation of typical amyloid fibrils.
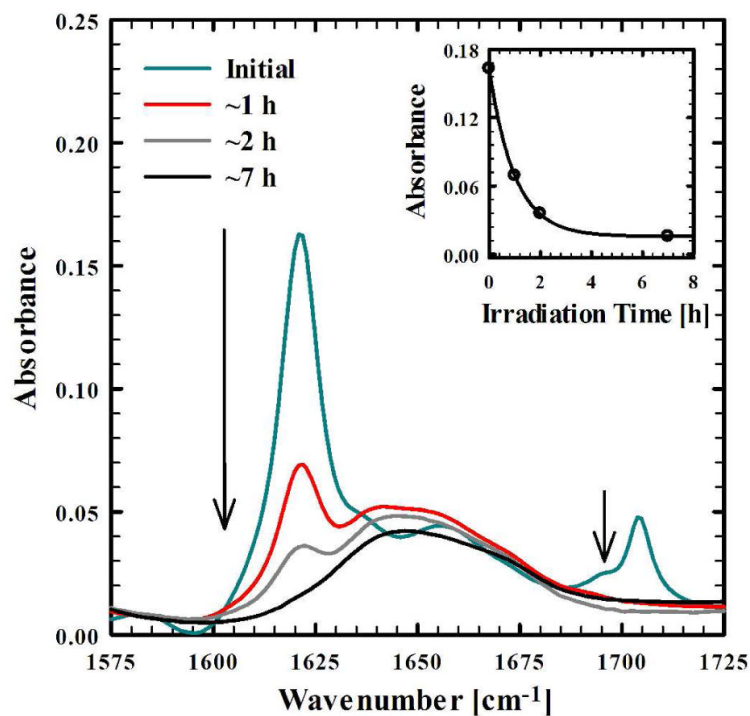
Figure 3.
FTIR spectra (in the amide I' region) of the F19K* aggregate solution in Figure 1, acquired at various times after irradiation with 355 nm light. The arrows depict the direction of increasing irradiation times. Also shown in the inset is the absorbance at 1620 cm^{-1} as a function of the irradiation time. The line is the fit of these data to a single-exponential function with a time constant of ~1 h.
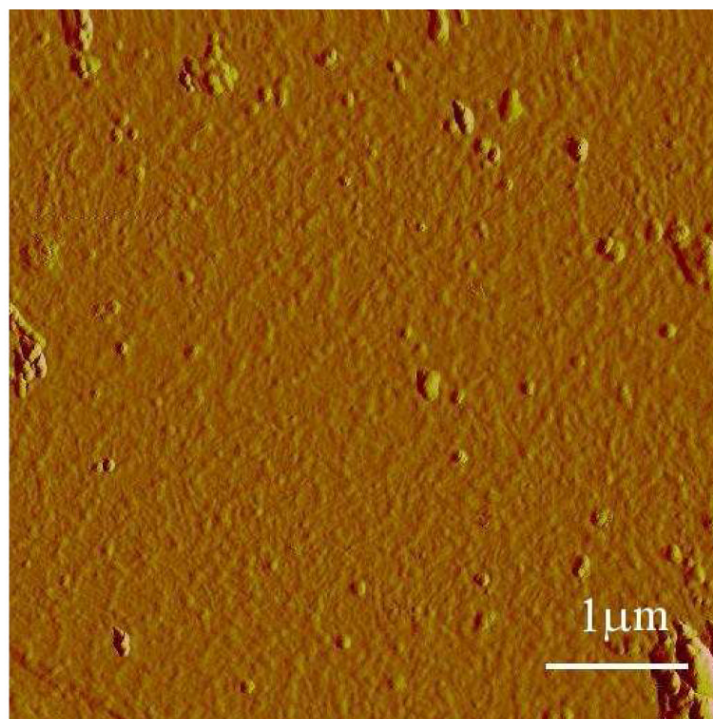
Figure 4.
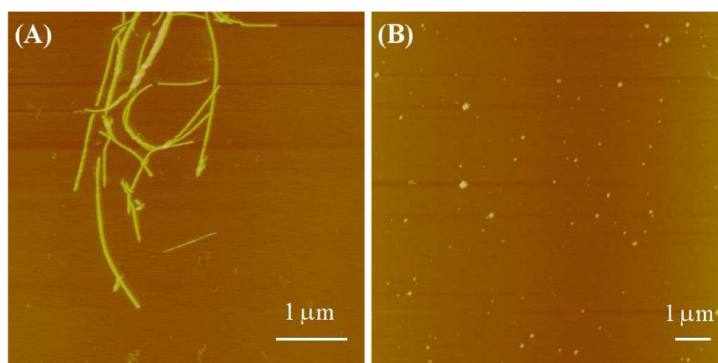A representative AFM image of the F19K* solution after 7 hours of irradiation.

Figure 5.
Representative AFM images of a ~500 µM peptide solution containing wild-type $A\beta_{16-22}$ and F19K*, at a molar ratio of about 1:1.5, (A) before and (B) after ~7 hours of irradiation.
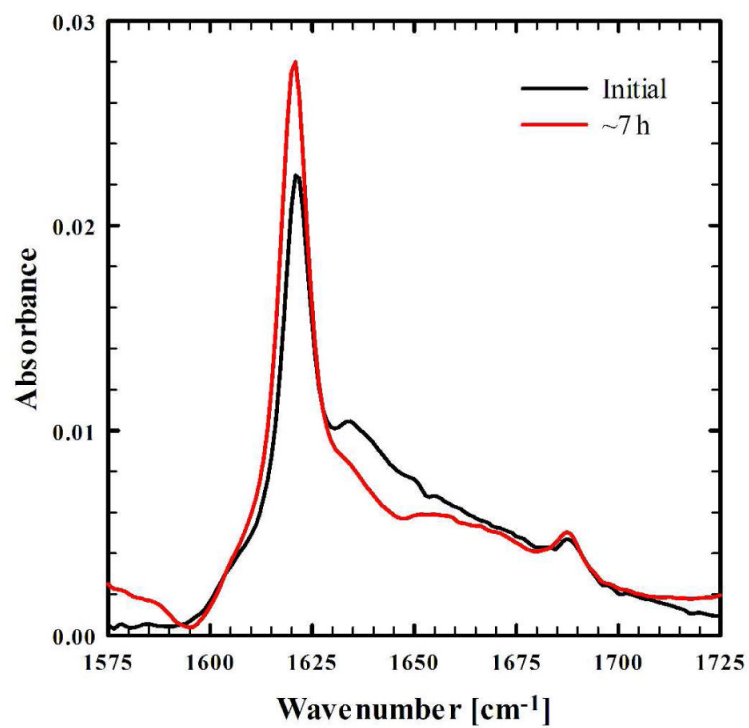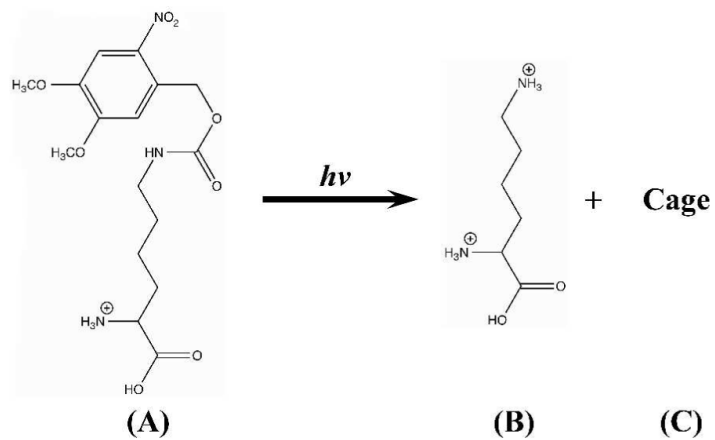
Figure 6.
FTIR spectra (in the amide I' region) of a 250 μM solution (pH 2) of a 3:1 mixture of K16K* and wild-type Aβ$_{16-22}$ with irradiation at 355 nm for the indicated amount of time. The comparatively lower concentration of the K16K* used herein was due to its poor solubility and higher aggregation propensity.

Scheme 1.
Irradiation of lys(Nvoc) (A) with near-UV light results in photocleavage of the Nvoc cage,
generating a charged lysine residue (B) and the cage photoproduct (C).